AD 661515

U. S. ARMY
TRANSPORTATION RESEARCH COMMAND
FORT EUSTIS, VIRGINIA

TRECOM TECHNICAL REPORT 64-6

SCALE MODEL AND FULL-SCALE VEHICLE TESTING IN COHESIVE CLAY SOILS

Task 1D021701A04901
Contract DA 44-177-TC-788

May 1964

prepared by:

SOUTHWEST RESEARCH INSTITUTE
Department of Automotive Research
San Antonio, Texas

55

NOTICES

When Government drawings, specifications, or other data are used for any purpose other than in connection with a definitely related Government procurement operation, the United States Government thereby incurs no responsibility nor any obligation whatsoever; and the fact that the Government may have formulated, furnished, or in any way supplied the said drawings, specifications, or other data is not to be regarded by implication or otherwise as in any manner licensing the holder or any other person or corporation, or conveying any rights or permission, to manufacture, use, or sell any patented invention that may in any way be related thereto.

* * * *

Qualified requesters may obtain copies of this report from

Defense Documentation Center
Cameron Station
Alexandria, Virginia 22314

* * * *

This report has been released to the Office of Technical Services, U. S. Department of Commerce, Washington 25, D. C., for sale to the general public.

* * * *

The findings and recommendations contained in this report are those of the contractor and do not necessarily reflect the views of the U. S. Army Mobility Command, the U. S. Army Materiel Command, or the Department of the Army.

HEADQUARTERS
U S ARMY TRANSPORTATION RESEARCH COMMAND
FORT EUSTIS, VIRGINIA

The U. S. Army Transportation Research Command concurs in the conclusions expressed by the contractor.

CARLO J. ROMA
Project Engineer

HERMAN P. SIMON
Group Leader
Land Transport Research and
Laboratory Operations Groups

APPROVED.

FOR THE COMMANDER:

LARRY M. HEWIN
Technical Director

Task 1D021701A04901
Contract DA 44-177-TC-788
TRECOM Technical Report 64-6

May 1964

SCALE MODEL AND FULL-SCALE VEHICLE TESTING IN COHESIVE CLAY SOILS

Report No. AR-506

Prepared by
Department of Automotive Research
Southwest Research Institute
San Antonio, Texas

for
U. S. ARMY TRANSPORTATION RESEARCH COMMAND
FORT EUSTIS, VIRGINIA

BLANK PAGE

TABLE OF CONTENTS

LIST OF ILLUSTRATIONS

LIST OF ILLUSTRATIONS (Cont'd)

LIST OF TABLES

INTRODUCTION

OBJECTIVE

The U. S. Army Transportation Research Command is engaged in a program to determine the feasibility of performing vehicular scale-model tests in natural terrains to predict the off-road performance of full-scale vehicles in all types of difficult terrain conditions such as snow, sand, marsh, muskeg, and clay soils. This report describes the investigation of full-size vehicle and scale-model performances in clay-type soils. The investigation included a dimensional analysis of soil and vehicle parameters that could function as significant factors in the correlation between model and full-size vehicle performance. The similitude theorem was employed in correlating prototype and model performance data.

TEST COURSES

Test courses were prepared in three different types of soils.

High-Cohesion Soil, CH, Silty-Clay

Clay-type soil having a high range of cohesion and "stickiness" or adhesion, located 7 miles west of San Antonio, adjacent to SwRI, was used for the first series of tests. The surface cover is a thin, stony soil several inches thick. An area at least 300 feet in length and 200 feet in width underlain by uniform, slightly sandy, fat black clay 4 feet or more thick was used for this investigation.

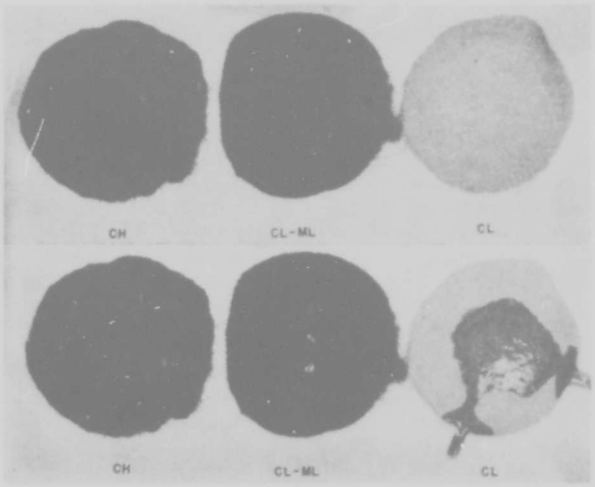

FIGURE 1. APPEARANCE OF THE TEST SITE SOILS

The material is a soil classified under Group Symbol CH, being a barely sandy, fat clay. The surface is mapped as Montell clay by the U. S. Soil Conservation Service. Liquid and plastic limits of this soil and the other two soils are shown in Figure 3, and grain sizes are shown in Figure 2 as defined by dry sieve and the hydrometer method. Figure 1, using particles of each type smaller than No. 20 mesh screen, illustrates the appearance of each soil.

Removal of a thin cover of oats, Johnson grass, and 2 to 3 inches of stony top soil was the first step in preparing this first site as a test course.

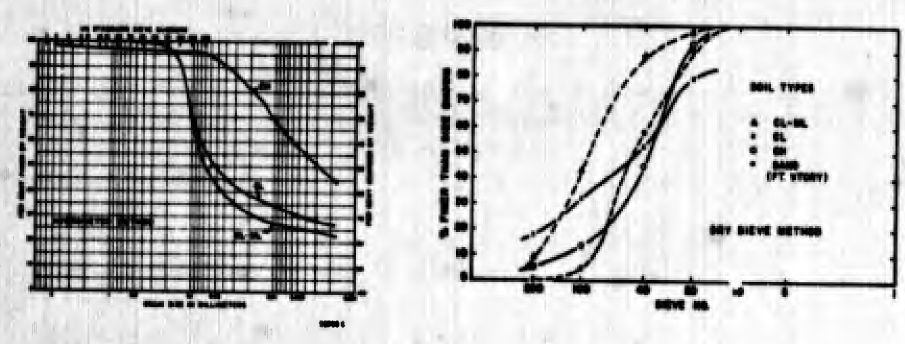

FIGURE 2. SOIL GRAIN SIZES IN TEST COURSES

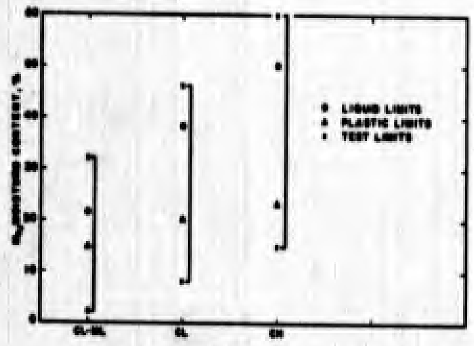

FIGURE 3. ATTERBERG LIMITS OF THE TEST SITE SOILS

Low-Cohesion Soil, CL-ML, Sandy Clay

The next site used for these tests contains a clay-type soil of low-range cohesion and adhesion located 8.2 miles east and 11.7 miles south of the center of San Antonio, in southeastern Bexar County, 2 miles west of Elmendorf. The test soil is a reddish-brown sandy clay, classified under the Group Symbol CL-ML, being a sandy clay or lean clay with low cohesion. The surface is mapped as Duval fine, sandy loam according to the U. S. Soil Conservation Service soils map.

Medium-Cohesion Soil, CL-Sandy Clay

Test course No. 3 had not been originally selected as a test site; but, in the course of examining the reddish sandy loam site, an additional soil type in the immediate vicinity was discovered. This site was at the bottom of the sandy loam hill described above, and a visual examination of the soil, both dry and wet, indicated sufficient difference in the two soils to justify conducting tests in this third soil. This soil has a higher percentage of clay and "fines" than the sandy soil CL-ML described above. One initial disadvantage of this soil was that it had been covered until just recently by 20 to 30 feet of overburden removed as fill material for a nearby dam. This caused the soil to be heavily compacted and much more difficult to disaggregate properly for the first few tests. Water slowly reduces this soil into a sticky, plastic clay, but it is less permeable than either soil CL-ML or soil CH. Note the water runoff in Figure 1.

This soil is a light brown to grey sandy clay classified under the Group Symbol CL. Figure 3 shows the Atterberg Limits of this soil to be approximately halfway between the other two test course soils.

SCOPE

The primary objective of this project was to establish correlation between the performance of full-size vehicles and scale models in clay-type soils by the use of the similitude theorem. Concurrently with the vehicle tests, an investigation was conducted into the basic soil parameters necessary for correlation and prediction of vehicle performance. The program was conducted chronologically as follows:

(1) Selection of suitable test sites and preparation of a similitude analysis.

(2) Instrumentation of test vehicles.

(3) Preparation of high-cohesion soil for vehicle and soil tests.

(4) Exploratory vehicle performance tests (Marsh Buggy and Marsh Buggy model) and calibration of instrumentation.

(5) Determination of soil parameters having the greatest effects on vehicle performance over the entire moisture content range.

(6) Vehicle performance tests and simultaneous soil tests in high-cohesion soil over a range of moisture content.

(7) Correlation analysis of test results in high-cohesion soil.

(8) Additional vehicle tests to "fill in" and substantiate performance trends in CH soil; in the Marsh Buggy and model at various weights, tire deflections, velocities, and tire types; and in the logistical cargo carrier model at two weights.

(9) Transfer of equipment to second test site.

(10) Vehicle tests, full size and models, in low-cohesion and medium-cohesion soils, including improved soil tests at varying moisture content.

(11) Effect of tire deflections, changing vehicle weight, and slip on tire sinkage and drawbar pull in low- and medium-cohesion soils (Marsh Buggy and Marsh Buggy model).

(12) Performance of logistical cargo carrier model and 3/4-ton cargo truck in low- and medium-cohesion soils.

(13) Analysis and correlation of all data, both vehicle and soil, by soil types.

PROCEDURE FOR FIELD EVALUATIONS

Normally, mobility problems are not encountered in clay-type soils that are very dry and/or hard; but this entire investigation (unless indicated otherwise) was conducted in disaggregated, leveled, and artificially irrigated soils. All soils were tilled to a depth of 18 to 24 inches and leveled just prior to the addition of water, and the vehicle and/or soil tests were conducted as soon thereafter as practicable after it had been established that the water had thoroughly distributed through the soil.

Soil samples for the determination of moisture content were taken from vehicle ruts as soon as a test was completed so that the sample would be representative of the soil exposed to the tire. In extremely wet soils where water was apt to settle into the bottom of the ruts, soil samples were obtained from the sides of the ruts. A similar procedure was used for obtaining soil samples for moisture content determinations in conjunction with soil tests.

The Marsh Buggy model, scaled 1 to 4.29 of the full-size prototype in the major linear parameters, was weighted to 650 pounds for comparison with the full-size vehicle weight of 11,990 pounds as follows

$K = 4.29$ (scaling factor)

$$\frac{11,990\#}{(4.29)^2} = \frac{11,990\#}{18.4} = 650 \text{ lb}$$

Model weight was varied from a minimum of 185 pounds to a maximum of 650 pounds. (Aluminum frame of model would not support a higher load.)

1/K was used for scaling pressure-penetratio plates for the determination of C_r. The diameters of the plates were 1.44 in. and 6 in.

DEFINITIONS

The definitions used in this report correspond wherever possible to previous TRECOM tests using this same equipment in sand and snow plus the inclusion of several developed to improve correlation of the data of this investigation.

1. Drawbar Pull, D. The load-towing capability of any powered vehicle expressed in pounds of force.

2. Vehicle Weight, W. The gross vehicle weight in pounds. To simplify the analysis of this investigation, the gross weight was always divided equally among the four wheels.

3. Diameter of Tire, d_w. Outside diameter of test vehicle tire, at zero deflection, measured in inches.

4. Width of Tire, b. Cross-sectional width of test vehicle tire measured at the widest point, at zero deflection, measured in inches.

5. Vehicle Velocity, V. The forward velocity of the test vehicle with respect to the ground, measured in feet per second.

6. Slip Ratio, S. The ratio of the test vehicle tire slip to the tire velocity

$$S = \frac{V_s - V}{V_s} \times 100$$

where

S = slip ratio, percent

V_s = tire velocity, feet/second (average of left and right rear tires with respect to a set of axes fixed on the vehicle)

V = vehicle velocity, feet/second

7. Tire Sinkage, Z. The average maximum depth of the tracks, measured in inches, left by a single pass of the vehicle in the test course.

8. Pass. One trip of the vehicle over the test course.

9. Liquid Limit, L_L. The moisture content at which the test soil, placed in a standard laboratory cup and grooved with a standard tool, will flow together for approximately 1/2 inch when jarred 25 times by raising the cup a prescribed distance (1 cm) and letting it fall. Soil characteristics are normally defined as changing from plastic to liquid at this percentage of water content.

10. Plastic Limit, P_L. The minimum moisture content at which crumbling occurs when a thread of soil is rolled to a diameter of 1/8 inch. The plastic limit is generally conceded to represent the moisture content at which a mixture of soil and water begins to take on plastic properties.

11. Plasticity Index, P_I. The numerical difference between the liquid and plastic limits. The numerical value of the plasticity index is some indication of the plasticity of the soil: highly plastic clays generally have high plasticity indexes; less plastic clays have lower plasticity indexes. This difference is sometimes referred to as the plastic range.

12. Moisture Content, M_n. The ratio, expressed as a percentage, of the weight of water in the soil to the dry weight of the solid particles in the sample.

13. Precollapse Structural Cohesion, C_S. The shearing resistance of the soil to the rotation of a round steel plate containing four radial vanes spaced 90° apart. See Figure 10. C_S was measured in the precollapsed or undisturbed (by test vehicles) soil of the test course.

Shear stress was calculated as follows, assuming uniform stress distribution over the circular area

$$C_S = \frac{3Q}{2\pi r^3}$$

where

C_S = shear stress, psi

Q = torque, inch-pounds

r = radius of plate, inches

14. Postcollapse Structural Cohesion, C_t. The shearing resistance of the soil (in the center of a test vehicle track) to the rotation of a circular vaned plate. C_t is calculated in the same manner as C_S.

15. Coefficient of Friction, f_n. The frictional resistance of the soil to the rotation of a loaded circular plate faced with neoprene rubber. This tends to simulate the action of a vehicle tire slipping and sinking in the test course. Frictional resistance, assuming uniform stress distribution over the circular area, was calculated as follows

$$f_n = \frac{3Q}{2\pi r^3 \sigma}$$

where

f_n = coefficient of friction

Q = torque, inch-pounds

r = radius of plate, inches

σ = normal unit loading, psi

16. Apparent Structural Cohesion, C_r. The relative load bearing characteristics of the soil measured by pressure-penetration tests of a series of circular plates. It is a measure of the sinkage of "modeled" plate diameters under a range of normal loadings. The slope of σ vs Z/d_p is compared to an arbitrary value of slope selected as unity. All other slopes, or C_r values, are referenced to this standard slope.

17. Precollapse Cohesion, C_c. The resistance of the soil to shearing by a rectangular shear plate pushed into the soil until the grousers are fully embedded. The soil is removed from the front of the plate in the direction that the force is applied. Breakaway force in pounds divided by the areas of the sides and bottom in square inches determines the cohesive strength in psi.

18. Postcollapse Cohesion, C_{ct}. The resistance of soil compacted by one pass of the test vehicle to shearing by the rectangular shear plate described above.

19. WES Cone Index, CI. The resistance of the soil to penetration by a cone penetrometer employing a 60° cone with a projected end area of 1/2 square inch.

20. Plate Penetration, Z_p. The sinkage of circular plates into the soil, measured in inches. Penetration is normally plotted as Z_p/d_p where d_p is the diameter of the plate. The subscript p is used to differentiate plate penetration from tire sinkage where both use the symbol Z.

21. Torque, Q. The force in inch-pounds required to maintain constant speed rotation of circular plates (both vaned and rubber faced) at various normal unit loads.

22. Angle of Internal Friction, ϕ. The effect of load on unit shearing resistance. The angle of internal friction, ϕ, is the tangent of the angle when plotting on a linear scale shear stress (ordinate) versus normal unit stress, using vaned plates.

23. Unit Loading, σ. This is the normal unit load, in psi, applied to various soil-parameter measuring devices.

24. Plate Diameter, d_p. The diameter, in inches, of circular soil-parameter measuring devices.

25. Sinkage Correction Factor, k_n. This is an empirically determined sinkage correction factor, where $Z_p/Z_m = k_n$. k_n is plotted as a function of moisture content and soil type.

EQUIPMENT

The following items of Government-furnished equipment were used during this investigation.

TEST VEHICLES

1. Prototype Marsh Buggy, Gulf (M.B.) Figure 4

   4 X 4 wheel drive

   114.7 in. X 38.5 in. smooth rubber tires

   Test weight, minimum, 11,990 pounds

   Test weight, maximum, 17,400 pounds

   Tread - 120 in.

   Wheel base - 150 in.

   Speed range - 3 to 17 ft./sec.

   Gasoline engine prime mover

   Differential in rear axle

   Front wheels chain-driven from rear wheels

2. Marsh Buggy Model (M.B. Model) Figure 4

   4 X 4 wheel drive

   25.9 in. X 9 in. smooth rubber tires

   Weight 185 to 650 pounds

   1 to 4.29 scale with prototype

   Tread - 24.8 in.

   Wheel base - 43.5 in.

   Hydraulic motor drive powered by Volkswagen engine mounted on dynamometer vehicle

   Flow divider between hydraulic motors and pump

   No differential

   Speed range - .5 to 1.5 ft./sec.

   Hydraulic steering

3. Marsh Buggy, Sandmaster (LARC Tires) (M.B. smt) Figure 5

   Weight - 10,640 pounds

   6 in. X 18.6 in. tires, 1/2 in. tread depth

FIGURE 4. PROTOTYPE MARSH BUGGY AND MARSH BUGGY MODEL WITH DYNAMOMETER VEHICLE (TERRAPIN) SOIL CH

FIGURE 5. LOGISTICAL CARGO CARRIER MODEL, 3/4-TON TRUCK AND MARSH BUGGY WITH SANDMASTER TIRES

4. Logistical Cargo Carrier Model (L.C.C. Model) Figure 5

   4 X 4 wheel drive

   1000-pound weight, minimum

   Differential locked (for test)

   Tread - 35.6 in.

   Wheel base - 75.0 in.

   Tires - 29.9 in. X 12 in., 1/4-in. tread depth

   Crosley engine mounted on model

   Hydraulic steering

5. Truck, Cargo, 3/4-Ton, M-37 (Truck, 3/4-Ton) Figure 5

   4 X 4 wheel drive

   Standard differential

   Weight - 6290 pounds

   Tires - 9.00 X 16, 5/8-in. tread

   Tread - 62 in.

   Wheel base - 112 in.

   Dodge gasoline engine

SUPPORT VEHICLES AND EQUIPMENT

1. 1-1/2-ton cargo truck with 1200-gallon water tank and portable pump

2. Two trailers, 2-wheel, with 500-gallon water tanks

3. Dynamometer and instrument vehicle (Terrapin)

   a. Dynamometer for controlling drawbar pull of test vehicles

   b. Contains power pack for M. B. model with controls

   c. Contains Palletized Soil Analyzer

   d. Contains recorder and controls for measuring both vehicle performance and soil characteristics

   e. All recording instrumentation

4. Tractor, full-tracked, D-8 Caterpillar, with bulldozer blade and gyrotiller for site preparation

INSTRUMENTATION

The instrumentation and controls used during this project are shown in Figures 6 and 7.

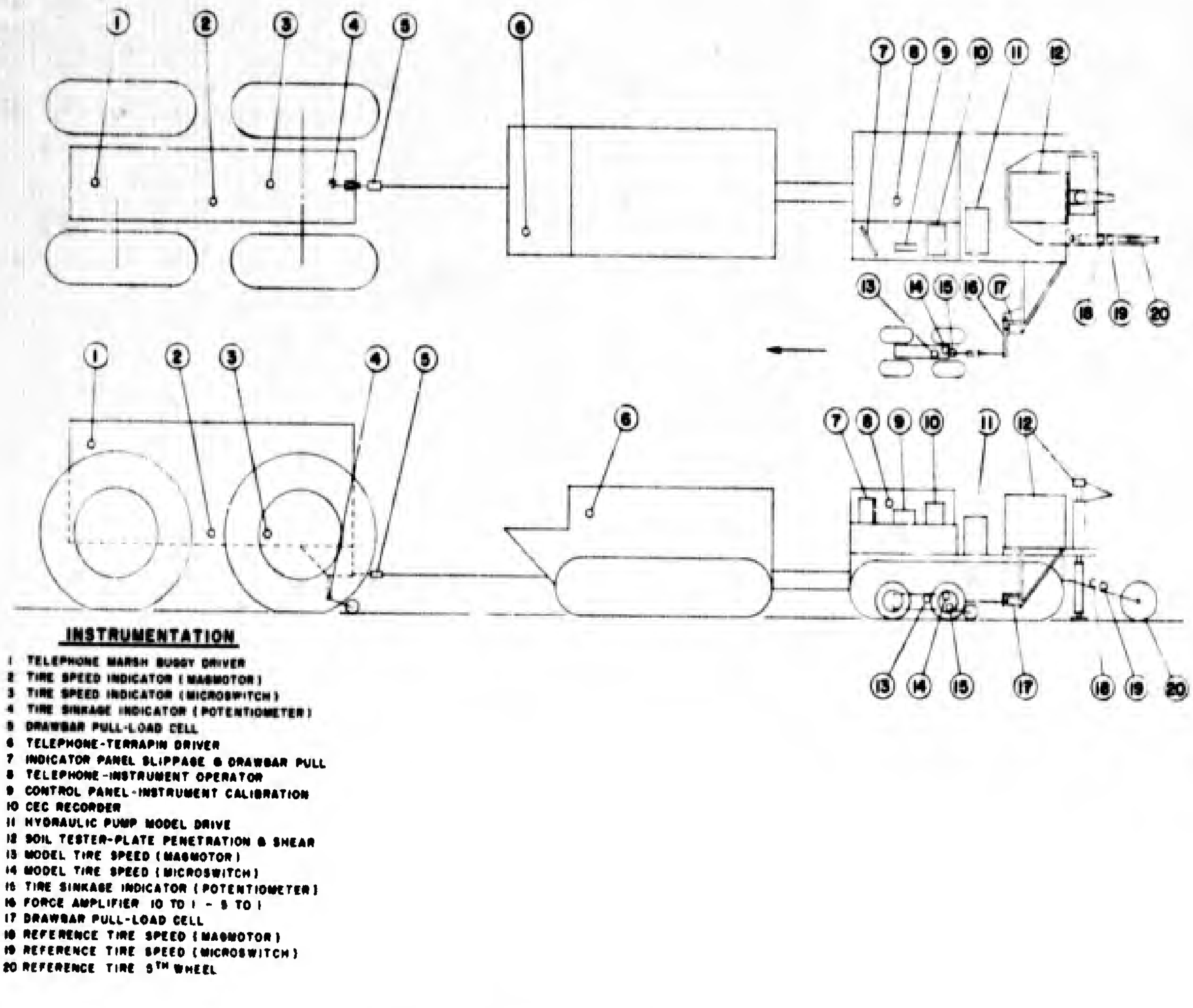

FIGURE 6. INSTRUMENTATION LAYOUT

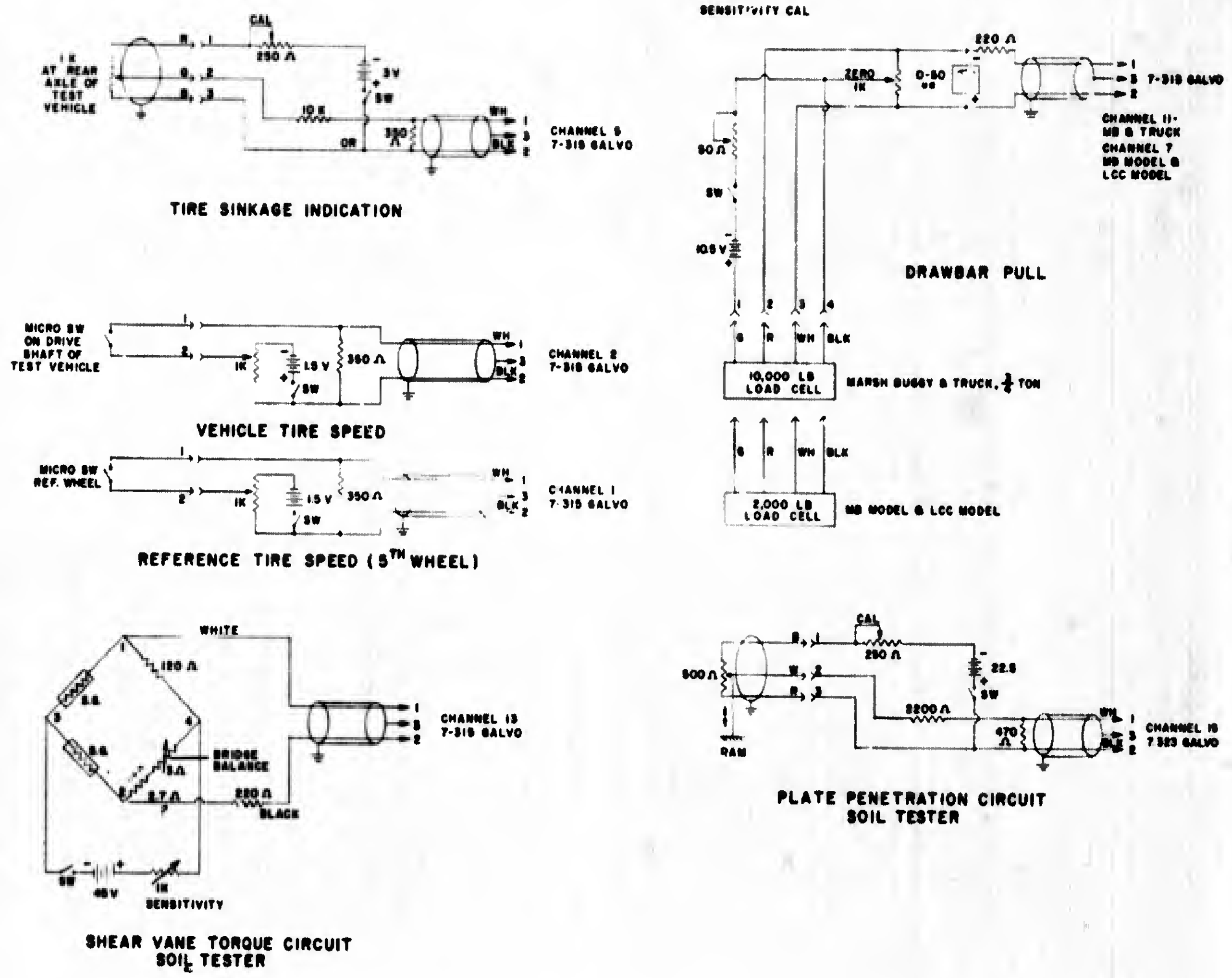

FIGURE 7. INSTRUMENTATION WIRING DIAGRAMS

TEST PROCEDURES

VEHICLE TESTS

A typical sequence of operations required to supply the baseline data on vehicle performance and soil characteristics as reported herein consisted of the following:

(1) Backdragging of a selected test course (20 feet wide by 200 feet long) with a D-8 tractor blade to remove weeds, grass, small stones, etc.

(2) Disaggregation of test course with several passes of D-8 tractor-driven gyrotiller to a depth of 18 to 24 inches. See Figure 8.

(3) Leveling of course with log pulled by 3/4-ton truck and 1-1/2-ton platform truck.

(4) Irrigating of staked portions of course by adding desired amounts of water (usually 1/3 as disaggregated, 1/3 damp, 1/3 wet). See Figure 9.

(5) Calibration checking of load cell by recording galvanometer deflection when applying known stress to cell. Recorder turned on for at least 30 minutes prior to calibration check.

FIGURE 8. PREPARATION OF TEST SITE WITH GYROTILLER SOIL CL-ML

FIGURE 9. IRRIGATING TEST COURSE, HIGH-COHESION SOIL CH

(6) Calibration checking of tire sinkage circuit by recording galvanometer deflection when raising sinkage wheel 5 inches and 10 inches.

(7) Checking operation of telephone, magmotor, and microswitch on test vehicles and reference wheel.

(8) Final briefing of vehicle drivers as to specific test conditions required; i.e., low slip, stop at changes of soil condition, or go-straight-through, etc.

(9) Turning on recorder at start of disaggregated test section.

(10) Proceeding through test course.

(11) Obtaining necessary soil samples from many different locations on test course (usually from or near vehicle ruts) for moisture content determination. Labeling of all samples as to location on test course.

(12) Measuring rut depth and location on course.

(13) Proceeding with individual soil parameter tests: C_s, C_t, C_r, C_c, C_{ct}, f_n and CI.

SOIL TESTS

Soil tests were conducted in the same test course immediately after completion of the vehicle tests. Soil samples were also obtained at regular intervals throughout these tests, as the soil moisture content sometimes changes rapidly (at least on top) in the disaggregated conditions, thereby quickly changing the soil characteristics. It was found to be practical during later stages of this investigation to prepare the test courses in the same manner as above, especially for soil characteristic determinations, by wetting down short sections (10 to 20 feet) of the course with progressively increasing amounts of water. One or at most two types of soil parameter tests were then conducted at a time, progressing through each section in turn. Thus, the effect of moisture content on any soil characteristic (such as friction or cohesion) could be carefully defined throughout the entire moisture content range. Moisture content was then used as a basic parameter for correlating vehicle tests and soil parameters.

Plate-Penetration Tests

Initial plate-penetration tests conformed to the procedures previously followed in TRECOM programs in sand and snow. That is, pressures and depth of plate penetration were simultaneously recorded using a constant rate of penetration. However, this method was unsatisfactory for disaggregated clay soils due to two reasons:

(1) The hydraulic loads were not repeatable at the same indicated pressures on the vertical cylinder of the soil analyzer, making accurate determination of loads difficult.

(2) The heterogeneous character of disaggregated clay soils made all penetration type tests of dubious value in predicting even average load-bearing capabilities of these soils. Penetration tests in "in situ" soils are of no value because of the variable levels of stratification and compaction in the natural "as is" soil.

To overcome the disadvantages of the bearing plate tester when used in these high-cohesion clay soils, plate penetration tests were subsequently conducted by directly loading circular plates by means of calibrated weights and recording sinkage as soon as the initial rate of penetration had essentially stopped. The solution to the second problem was not so easy; all plate penetration tests were repeated many times to obtain the average results reported herein, but the normal spread in test data produced as much as a 5:1 ratio between sinkages measured at the same time in the same soil with the same vertical load. Even the average values do not appear to be representative of the actual soil characteristics. For example, a small-diameter plate may contact a large, hard clod of clay, whereas a larger diameter plate near the same location may contact only fully disaggregated soil.

Cone Penetrometer Tests

The cone penetrometer tests consisted of pushing a 60-degree steel cone into the ground and recording the resistance of the soil to a preselected depth of penetration by the cone. Hundreds of cone penetrometer tests were conducted in the three types of soil throughout the applicable moisture content range.

Grid Plate Tests

The grid plate tests consisted of determining the maximum internal cohesive strength of the soil by measuring the resistance offered to horizontal movement of a rectangular plate pushed into the ground. The grid plate, illustrated in Figure 10, is 10 inches long, 5 inches wide, and 2 inches deep, and did not have a normal unit load. The postcollapse strength, C_{ct}, of the soil was measured in the tracks of the Marsh Buggy and the Marsh Buggy model.

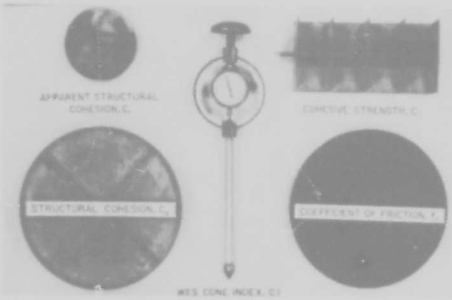

FIGURE 10. SOIL ANALYSIS EQUIPMENT

Shear Vane Tests

The resistance of the soil to rotation of loaded circular vaned plates, commonly used, were 5.6 inches in diameter and 11.2 inches in diameter. The depth of the vanes was 1/2 inch. Constant normal unit loads were applied to the plate, and rotational speed was held constant. Torque, penetration, and elapsed time were recorded. When these high-cohesion soils displayed definite fluctuations of resistance due to its stick-slip frictional characteristics, maximum torque values were plotted.

Rubber-Faced Plate Tests

The frictional characteristics of the soil were determined by substituting neoprene rubber-coated plates for the vanes described above and using identical test procedures. 5.2-inch diameter and 11.2-inch diameter plates were used. Torque, penetration, and elapsed time were recorded with the normal unit loading and rate of rotation maintained at a constant level. Maximum torque was plotted where large fluctuations of torque were recorded in high-cohesion soils. Torque values and plate penetrations were determined at the start of rotation (breakaway) and at 1 second, 2 seconds, 5 seconds, and 10 seconds after start of rotation. The averages of these readings are plotted in this report unless indicated otherwise.

RESULTS

Unless indicated otherwise, the Marsh Buggy model and prototype results are always based on the following baseline values: 11,990-pounds gross weight with the standard large tires and the Marsh Buggy model scaled to 650 pounds. Tire deflections for both vehicles was maintained at 12 percent for all gross weights. The other three vehicles were tested at normal tire pressures.

SOIL CH - HIGH-COHESION SILTY-CLAY

Vehicle Test Results

The results of a large number of vehicle tests, in all three soils tested, are shown in Table II. Each of these tests, unless indicated otherwise, is the average of three or more observed data points.

Since the objective of this program was to determine the feasibility of correlating scale model to prototype vehicle performance through proper scaling factors, the results shown on Figure 11 are of primary interest. Excellent correlation between the Marsh Buggy model and the Marsh Buggy prototype is shown at 30-percent slip ratio. D/W, the drawbar pull coefficient, and f_n, the coefficient of friction of the soil, are plotted as functions of moisture content. The matching of these curves with maximums and minimums falling at almost identical moisture contents indicates clearly that the drawbar pull is strongly influenced by the coefficient of friction of the soil. All other means of plotting the data, using the various Pi terms evolved in the dimensional analysis shown in Appendix II, failed to demonstrate any degree of correlation.

D/W, for the Marsh Buggy using Sandmaster tires, is also shown on this figure. These tires raise the drawbar pull coefficient slightly at the lower moisture contents but drop sharply below the larger cross section smooth tires as the moisture content approaches the liquid limit and the coefficient of friction, f_n, of the soil drops to a low value.

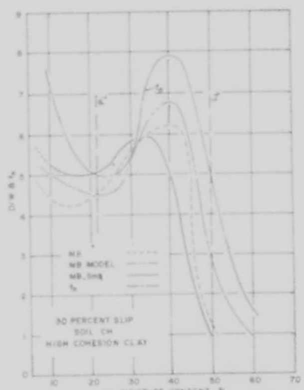

FIGURE 11. DRAWBAR PULL AND SOIL FRICTION, LOW SLIP, SOIL CH

FIGURE 12. MARSH BUGGY IN HIGH-COHESION SOIL CH

The sharp peak, or maximum D/W, shown at approximately 40 percent moisture content, results from "stickiness" or adhesion of the clay to the tires in this relatively narrow band of moisture content. This "stickiness" effect or adhesion to the tires is demonstrated dramatically in Figures 12 and 13, showing the clay clinging to the surface of the tire. Conventional tire parameters become somewhat meaningless when this condition is encountered. The difficulty of making accurate and effective soil measurements at this soil condition is clearly shown in Figure 14, where the clay is shown "balled up" completely around one of the rubber-faced plates used for measuring f_n. However, this adhesion to the plates is duplicating the effect shown in both Figures 12 and 13, where it is clinging to the surface of the tires.

FIGURE 13. MARSH BUGGY MODEL IN HIGH-COHESION SOIL CH

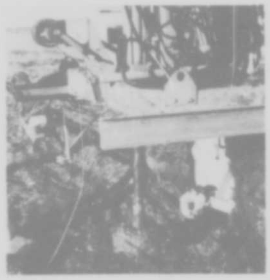

FIGURE 14. APPARATUS FOR DETERMINATION OF SOIL COEFFICIENT OF FRICTION IN SOIL CH (HIGH MOISTURE CONTENT)

Figures 15 and 16 show the passage of the Marsh Buggy prototype and model, respectively, in a mid-range moisture content prior to initiation of the full adhesion effect. The soil in the rut is rippled from some pickup of the soil by the tire, yet there is no adhesion to the tire itself. Note the low sinkage, Z, in those ruts and the large amount of sinkage shown in Figure 12. Despite the large sinkage shown in Figure 12, the drawbar pull is possibly 50 percent greater than the drawbar pull attained with the low sinkage shown in Figure 15. This, then, demonstrates that correlation of drawbar pull as some function of the sinkage is not feasible in this soil.

FIGURE 15. TEST COURSE AFTER ONE PASS OF MARSH BUGGY WITH SANDMASTER TIRES, SOIL CH (MEDIUM MOISTURE CONTENT)

FIGURE 16. TIRE TRACKS OF MARSH BUGGY MODEL IN SOIL CH

Of the greatest significance in conducting tests in this type of soil and in correlating the results is a change in D/W by a factor of 5 or 6 with a change in moisture content of only 10 percent. Meticulous soil preparation and moisture distribution on the course are necessary to produce repeatable results. Only a few percent of moisture content variation on either side of the critical moisture content range causes the CH soil to rapidly lose its adhesive properties and to lose the high D/W value attained when this high level of adhesion occurs.

Figure 17 illustrates good correlation between model and prototype at 70 percent slip. Better correlation at the maximum D/W point at 40 percent moisture content might have resulted if it had been possible to obtain D/W values of greater than .65 on the Marsh Buggy prototype, but drive chain breakage occurred at higher D/W values than this. At this high slip ratio there is another factor that could have contributed to lower D/W values for the prototype: differential slippage of the wheels. The model had a locked differential and the prototype had a free differential. At the higher values of slip ratio this caused the tires on one side of the prototype to speed up and the tires on the other side to slow down, thereby providing a distorted value for the true slip ratio.

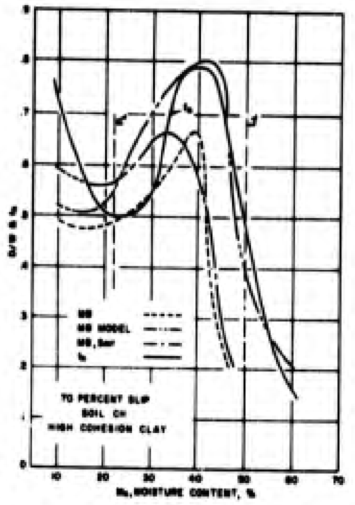

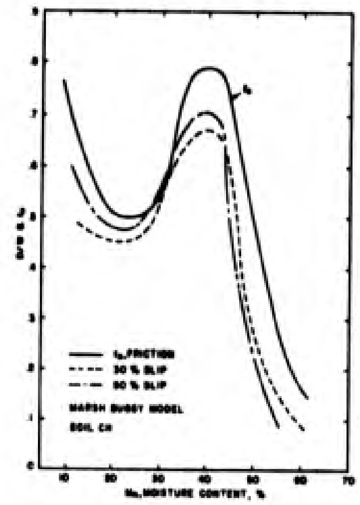

FIGURE 17. DRAWBAR PULL AND SOIL FRICTION, HIGHSLIP, SOIL CH

FIGURE 18. EFFECT OF SOIL MOISTURE CONTENT ON DRAWBAR PULL IN SOIL CH, MARSH BUGGY MODEL

Figure 18 illustrates the variation of D/W for the Marsh Buggy model for two values of slip ratio over the entire moisture content range tested. Again the curves have maximums and minimums at the same moisture content levels and display a similarity to the f_n values over this range.

Figure 19 shows the tire sinkage parameter, Z/d_w, as a function of moisture content. The Marsh Buggy prototype did not show any appreciable increase in sinkage until it reached the liquid limit of the soil; however, the model started to increase its sinkage midway between the plastic limit and the liquid limit.

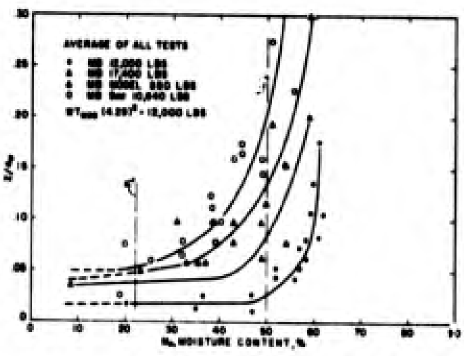

FIGURE 19. EFFECT OF SOIL MOISTURE ON TIRE SINKAGE IN SOIL CH

Although the modeling technique does not appear to offer good correlation at this point, it is evident that the shapes of the curves are similar. Multiplying the values of Z for the model by a correction factor appears to provide a reasonable level of correlation; therefore, it appears that the absolute value of $Z_{prototype} = k_n Z_{model}$. See Figure 46.

SOIL CL - MEDIUM-COHESION SANDY-CLAY

In this medium-cohesion clay, the model and prototype again demonstrated good correlation. Figure 20 shows D/W versus moisture content plotted for four vehicle configurations and f_n, the coefficient of friction of the soil. The peak D/W values for the model are not as well matched to the Marsh Buggy at this soil condition, but the Marsh Buggy again demonstrated excellent correlation with the f_n curve.

The Sandmaster tires on the Marsh Buggy demonstrated close performance to the large-diameter smooth tires. Near the plastic limit, the Sandmaster tires have slightly improved performance, but the drawbar pull drops off faster for the smaller tires midway between the plastic and liquid

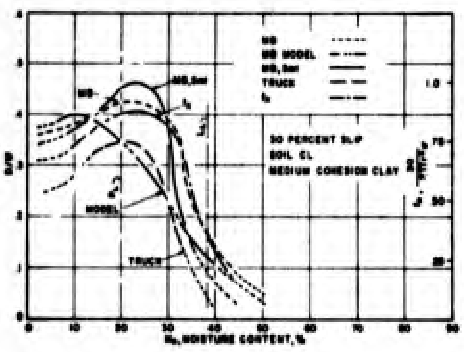

FIGURE 20. CORRELATION BETWEEN DRAWBAR PULL AND SOIL FRICTION LOW SLIP, SOIL CL

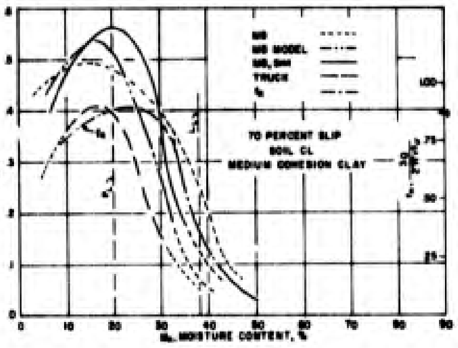

FIGURE 21. CORRELATION BETWEEN DRAWBAR PULL AND SOIL FRICTION HIGH SLIP, SOIL CL

limits of the soil. The 4 X 4, M-37 truck demonstrated somewhat reduced D/W values throughout the range, but the shape of the curve is similar to the f_n and the Marsh Buggy curve.

Figure 21 illustrates the 70-percent slip ratio or high slip condition in this medium-cohesion clay. The model and prototype demonstrated similar D/W curves with the maximum D/W at the same moisture content level, but the model shows lower D/W values at moisture contents above the plastic limit. However, the slopes and shapes of the two curves are quite similar throughout the moisture content range. Again, the M-37 truck demonstrated lower D/W values but a drawbar pull curve that is identical in slope and position on the moisture content range to the Marsh Buggy performance curve. The Sandmaster tires demonstrated slightly improved drawbar pull as compared to the large-diameter smooth tires at or near the plastic limit of the soil, but this advantage was quickly lost midway between the plastic and liquid limits of the soil. At this slip condition, in this soil, the vehicles demonstrated greater divergence from the moisture content value at which the f_n values showed a maximum value. However, the Marsh Buggy, with Sandmaster tires, did show a peak D/W value at a moisture content within 1 to 2 percent of the moisture content for the peak f_n values.

This particular CL clay soil has unusual characteristics that differ markedly from the CH soil, the high-cohesion clay, used at the first test site. This soil was difficult to disaggregate by mechanical tilling action, and it exhibits a low permeability to water. The soil increases in cohesion, adhesion, and load-carrying capacity up to approximately 25-percent moisture content; it then drops off rapidly as the moisture content approaches the liquid limit.

Figure 22 illustrates the water retention characteristics of the CL soil as the test course is being prepared for the Marsh Buggy model. Figure 1 also illustrates the water retention characteristic of the soil. Although water was poured on all three samples of soil at essentially the same time, the water is standing on top or flowing off the CL soil sample, but it has soaked into the other two samples.

Figure 22 is representative of a typical test course layout in that three levels of moisture content are being established on the course. The short test course as shown in this photograph could be used for the model and still obtain stabilized conditions. The vehicles always approached the test course from the dry end to prevent carry-over of moisture into the lower moisture content region.

Figure 23 illustrates the sinkage experienced by the various vehicles over the moisture content range. As in the CH soil, the model shows a higher Z/d_w value than the prototype, although the shapes of the two curves are similar. Of interest is the sinkage of the Marsh Buggy 50-percent overload, which is almost identical to the normal 12,000 pounds gross weight condition.

Figure 24 shows the comparison between C_s and f_n in the CL soil. C_s, for the 11.2-inch diameter vane, demonstrates an improved correlation with D/W in this soil, although it does not exhibit the sharp drop of f_n and D/W, shown in Figure 20, as the liquid limit of the soil is approached.

FIGURE 22. PREPARATION OF SOIL CL FOR VEHICLE TEST

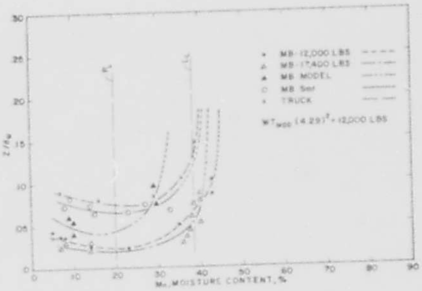

FIGURE 23. EFFECT OF SOIL MOISTURE ON TIRE SINKAGE, SOIL CL

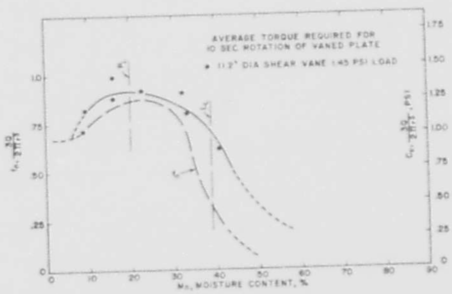

FIGURE 24. EFFECT OF SOIL MOISTURE CONTENT ON COHESION (VANED ROTARY PLATE) IN SOIL CL

SOIL CL-ML - LOW-COHESION SANDY-CLAY

This soil was a difficult medium to employ for correlation purposes. The narrowness of the plasticity index placed an extreme premium on the homogeneity of water distribution throughout the test course. Figures 25 and 26, slip ratios of 30 percent and 70 percent, respectively, illustrate the steep slopes of the D/W and f_n curves at or near the liquid limit. As in previous soils, the f_n curve shows good correlation with the Marsh Buggy D/W curve at this 30-percent slip ratio, but the peak of the Marsh Buggy curve is displaced toward a lower moisture content level at the higher slip ratio. Reasonably good correlation is obtained between the model and prototype at both slip ratios, but the peak D/W value for the model tends to be displaced toward an 8 to 10 percent lower moisture content level than the prototype. The maximum D/W values show good agreement, although the prototype shows slightly higher D/W values for both slip ratios, a reversal from the CH soil. The sinkage for the various vehicle configurations is shown in Figure 27. As in the other soils, the sinkage response parameter, Z/d_w, follows the same curve shapes with minimum values and slopes in good agreement; however, the model sinkages must be divided by a correction factor to bring the Z/d_w values into reasonable agreement. Again it appears that $Z_p = k_n Z_m$. Unlike the Z/d_w values in the CL soil, the 50-percent overload on the Marsh Buggy significantly increases the sinkage.

The 3/4-ton M-37 had the highest Z/d_w values as well as the highest ground-pressure loading values. Figure 28 illustrates the sinkage of the M-37 when it became immobilized at a moisture content close to the liquid limit of this soil.

The approximate ground pressures of each vehicle are shown in Figure 29 for 70-percent slip. The full-scale vehicles indicate a trend of higher sinkage for higher unit ground pressures, but the models show disproportionately higher Z/d_w sinkage values. Referring to Figure 26, it is possible to see that the D/W values for these vehicles in the moisture range shown for Figure 29 are relatively close and do not reveal the wide spread of values shown by the Z/d_w sinkage parameter.

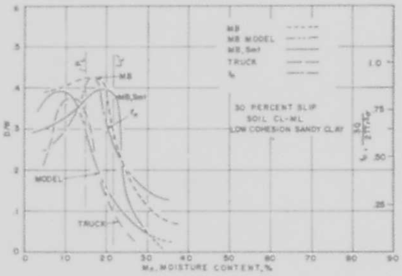

FIGURE 25. CORRELATION BETWEEN DRAWBAR PULL AND SOIL FRICTION, LOW SLIP, SOIL CL-ML

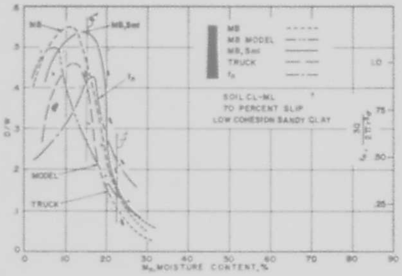

FIGURE 26. CORRELATION BETWEEN DRAWBAR PULL AND SOIL FRICTION

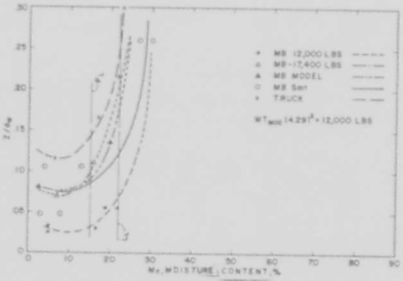

FIGURE 27. EFFECT OF SOIL MOISTURE ON TIRE SINKAGE, SOIL CL-ML

FIGURE 28. THE SINKAGE OF 3/4-TON TRUCK IN SOIL CL-ML AT THE LIQUID LIMIT, 25% MOISTURE CONTENT

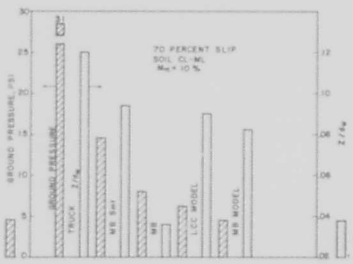

FIGURE 29. EFFECT OF TIRE GROUND PRESSURE ON SINKAGE

FIGURE 30. RELATIVE SIZES OF TEST TIRES

The relative size of the various tires used on the various vehicle configurations is shown in Figure 30. The tires from top to bottom are:

(1) Marsh Buggy Model Tire

(2) Logistical Cargo Carrier Model Tire

(3) 3/4-Ton, M-37 Truck Tire

(4) Marsh Buggy Sandmaster Tire

(5) Marsh Buggy Standard Tire

Figure 31 illustrates the C_s and f_n values measured over the moisture content range. C_s does not duplicate the sharp slope of f_n and D/W as the liquid level of the soil is approached.

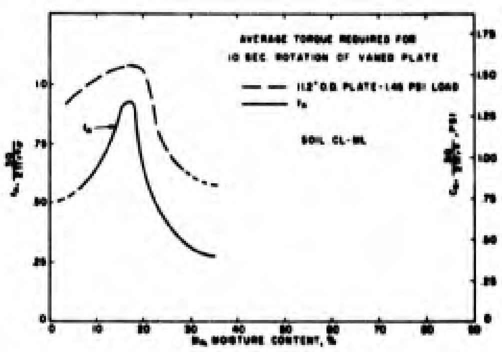

FIGURE 31. EFFECT OF SOIL MOISTURE CONTENT ON COHESION IN SOIL CL-ML

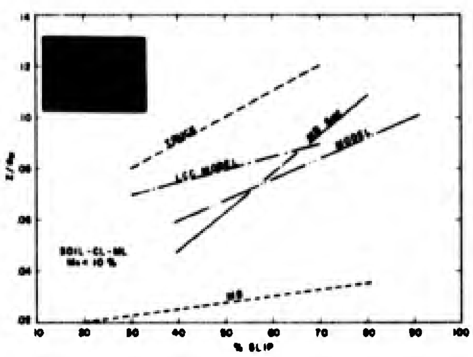

FIGURE 32. EFFECT OF SLIP ON TIRE SINKAGE

Figure 32 presents Z/d_w versus slip ratio for the five vehicle configuration tested in the CL-ML soil. The soil is at less than 10-percent moisture content and is therefore below the plastic limit of the soil. The lower sinkage of the large-diameter Marsh Buggy tires is revealed clearly in this graph.

Figure 33 presents a number of plate sinkage determinations in the CL-ML soil. This is typical of the wide scatter of data points obtained in determining C_r values in the three soils. Nonhomogeneity of the disaggregated test course soils can mask any latent effects of the soil that may manifest their presence in a completely homogeneous soil.

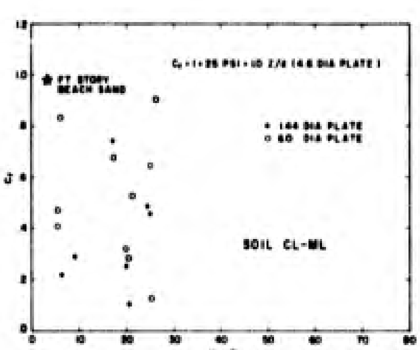

FIGURE 33. VARIATIONS IN C_r OBTAINED FROM PLATE PENETRATION TESTS IN TILLED SANDY SOIL CL-ML

COMPARISON OF CH, CL, and CL-ML SOILS

The steepness of the D/W and Z/d_w curves in all three soils near the liquid limit can be explained by Figure 34, which shows the liquid limit determinations of the three soils. It is significant that the slopes of the f_n and D/W curves versus moisture content for any given vehicle at or near the liquid limit in one of these soils show the same relative sensitivity to moisture content as demonstrated by Figure 34.

One of the parameters to be studied in this investigation was the effect of vehicle gross weight on L/W. Figure 35 demonstrates that in two of the soils studied, that vehicle weight does not have an appreciable effect on D/W. In the CL soil, the sinkage was relatively unaffected by gross weight; however, in the CL-ML soil, the sinkage increased noticeably for a 50-percent increase in gross weight. The scatter of data points at the 20- and 25-percent moisture content curves for the CL-ML soil can possibly be explained by the extreme sensitivity of this soil to moisture content at this level because these values are on either side of the liquid limit. A larger sampling cross section at these moisture content levels at the mid-range gross weight will possibly raise this point to "flatten out" this D/W curve.

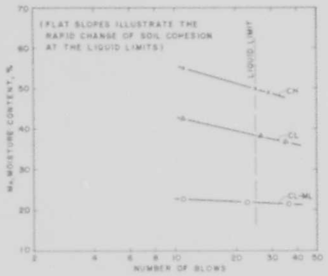

FIGURE 34. LIQUID LIMIT DETERMINATIONS OF TEST COURSE SOILS

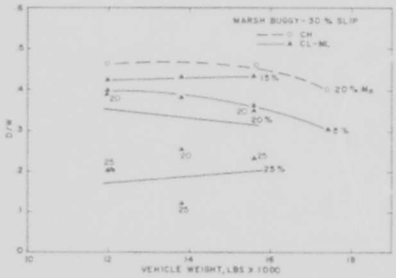

FIGURE 35. EFFECT OF GROSS WEIGHT OF VEHICLE ON DRAWBAR PULL

Figure 36 illustrates the means employed to vary the gross weight of the Marsh Buggy. The frame of the Marsh Buggy could not resist extra loading; therefore, special valves were constructed to pump water into the tires to increase the gross weight of the vehicle and still permit control of the air pressure. Multiples of 55 gallons of water were pumped into each tire to vary the gross weight, and this was accomplished rapidly and inexpensively at the remote test sites with a minimum of handling problems.

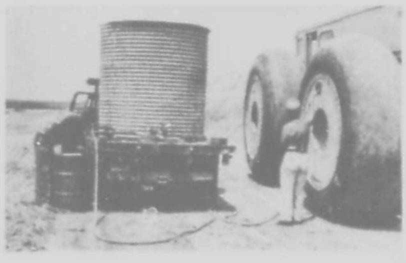

FIGURE 36. INCREASING WEIGHT OF MARSH BUGGY

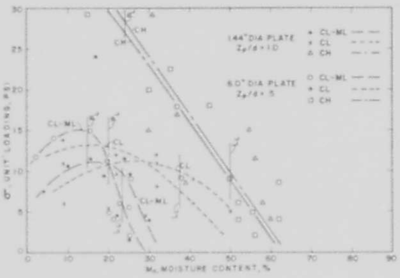

FIGURE 37. LOAD-CARRYING CAPACITY OF TEST SOILS

Figure 37 illustrates the unit loading, σ, to sink two plates with diameters of 1.44 inches and 6.0 inches to a value of $Z_p/d_p = 1.0$ and $Z_p/d_p = 0.5$, respectively, for the two plates. Of all of the load-carrying-capacity curves developed in the three soils, the values shown for both sizes of plates developed in the low-cohesion CL-ML soil are the only two curves bearing any resemblance to the D/W versus moisture content curves generated for the various vehicle configurations. This is understandable, however, because the load-carrying capacity of the terrain provided good correlation with the D/W developed when the values were measured in sand in previous studies. The CL-ML soil approaches sand in its composition, consistency, and homogeneity. It is evident from analyzing this figure that in studying high-cohesion soils, little or no dependence can be placed in extrapolating values obtained from load-bearing tests to predict drawbar pulls in these soils.

The Cone Penetrometer Index for 5 inches of penetration for all three soils is plotted on Figure 38. For the high-cohesion soil, CH, the Cone Index indicates that maximum drawbar pull could be expected in the driest possible soil. The Cone Index does indicate a sharp loss of mobility beyond the liquid limit; however, it does not show the 4 or 5 to 1 reduction in drawbar pull that results in the band between 40- and 50-percent moisture content. In fact, it indicates only a minor reduction in traction in this range.

The Cone Index reveals improved correlation with D/W versus moisture content for the medium- and low-cohesion soils, CL and CL-ML. The moisture content level at which the peak D/W values

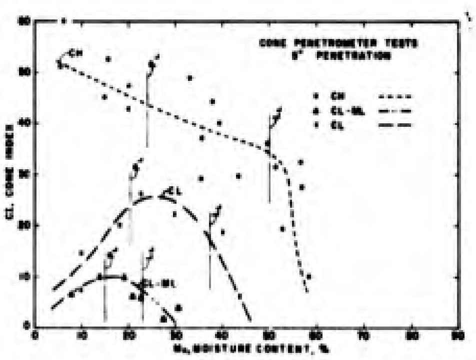

FIGURE 38. EFFECT OF MOISTURE CONTENT ON CONE INDEX

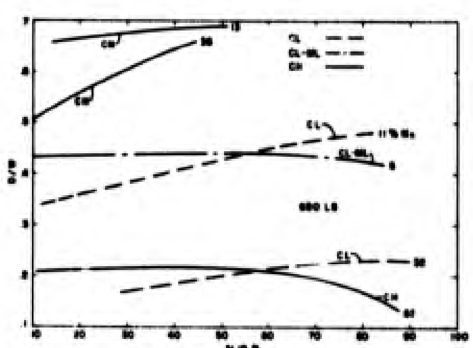

FIGURE 39. EFFECT OF SLIP ON DRAWBAR PULL MARSH BUGGY MODEL, THREE SOILS

were obtained is correlated well by the Cone Index value, but a sharp dropoff of traction near the liquid limit is not indicated. The relative maximum values of D/W are not indicated by the Cone Index when comparing the three soils, that is:

	Values at Same Moisture Content	
Soil	Max. D/W (Marsh Buggy)	Cone Index
CH	.62	38
CL	.42	26
CL-ML	.42	10

Figure 39 demonstrates only a small shift in D/W as a function of slip ratio for a given soil and moisture content. In the high-cohesion soil, CH, there is a tendency to lower the drawbar pull at the higher slip ratios at a moisture content beyond the liquid limit of the soil.

Figure 40 is presented to show the results obtained with the rectangular grid plate for determining the cohesion of the soil. The value C_c, the precollapse cohesion of the soil, was measured in the undisturbed soil. C_{ct}, the postcollapse cohesion, was measured in the compacted soil at the bottom of the rut created by one pass of the Marsh Buggy. The curve does not show any significant trends that can be correlated to the variation of D/W or Z/d_w as a function of moisture content.

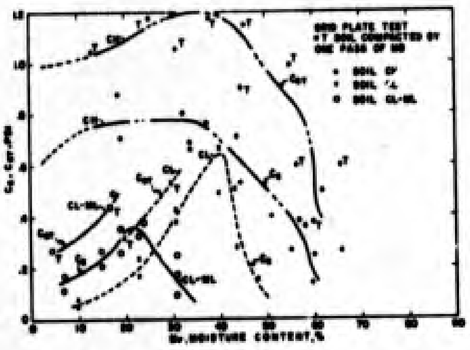

FIGURE 40. EFFECT OF SOIL MOISTURE CONTENT ON COHESION (GRID PLATE) OF TEST COURSE SOILS

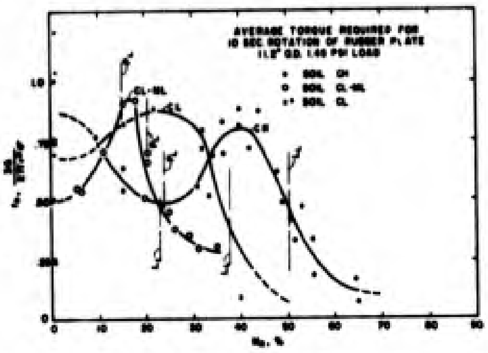

FIGURE 41. EFFECT OF SOIL MOISTURE CONTENT ON SOIL COEFFICIENT OF FRICTION

For comparison, Figure 41 shows f_n plotted as a function of moisture content for all three soils. Of particular interest in the case of the high-cohesion soil, CH, is the increase of f_n at lower moisture content level after dropping to a reduced level at the plastic limit. Neither of the other two soils indicated this tendency.

Figure 42 is included as a matter of academic interest. In obtaining the f_n values by rotating the 11.2-inch diameter rubber-faced plate, the penetration during 10 seconds of rotation was recorded. This was one of the many soil parameters studied in a search for correlating factors. The "cross-over" of the CL (medium-cohesion soil) over the CH (high-cohesion soil) near the liquid limits of CL soil may be explained by its low permeability to water. It may have developed a lubricating layer of water between the soil and the rubber to reduce migration of the soil to the outer perimeter of the rotating plate.

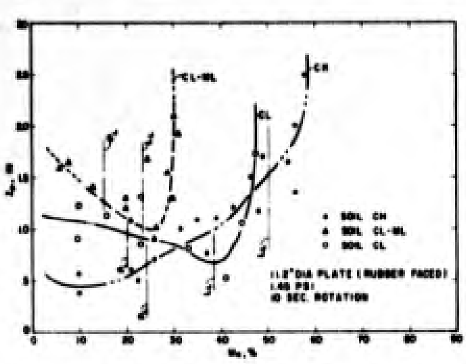

FIGURE 42. EFFECT OF SOIL MOISTURE CONTENT ON SOIL LOAD-BEARING CHARACTERISTICS

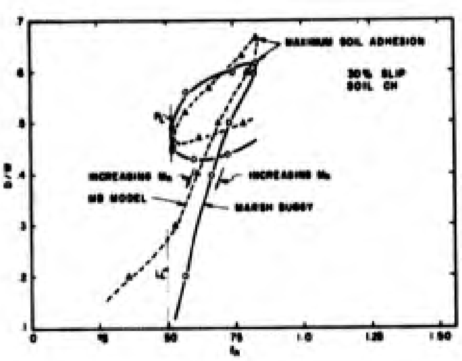

FIGURE 43. DRAWBAR PULL VS. SOIL FRICTION, HIGH-COHESIVE CLAY CH

Figures 43, 44, and 45 illustrate the D/W for the Marsh Buggy and model plotted as a function of f_n. The prototype and model illustrate the best correlation in the region of maximum D/W and maximum adhesion of the soil. The "loop" in the D/W versus f_n curve, plotted in the direction of increasing moisture content, has the most predominant loop with the CH soil of high cohesion. It is evident that this effect could be the result of the higher adhesion characteristics of this soil. The best correlation between the model and prototype is obtained in soils having the highest plasticity index in the moisture content range where D/W versus M_n shows the lowest slope. Increasing the slope of the D/W versus M_n curves results in a greater spread in the model and prototype curves because of the increased sensitivity of the vehicles to the moisture content of the soil. Increased sensitivity of the vehicles to moisture content results in an increased probability of the scale-model vehicle's being affected by stratification of the water in layers near the surface of the soil. This is

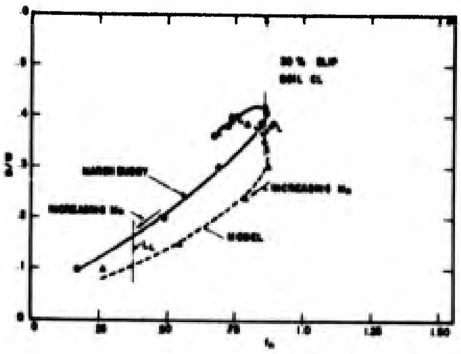

FIGURE 44. DRAWBAR PULL VS. SOIL FRICTION, MEDIUM-COHESION CLAY, CL

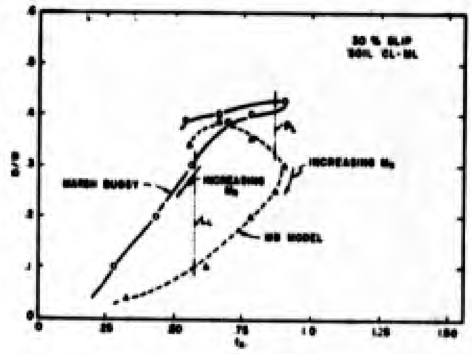

FIGURE 45. DRAWBAR PULL VS. SOIL FRICTION, LOW-COHESION CLAY, CL-ML

borne out by the tendency of the model to have lower D/W values at the higher moisture content levels in the lower-cohesion soils.

Figure 46 illustrates the sinkage factor, k_n, plotted as a function of moisture content for the three soils at two different scaling weights for the prototype, 12,000 and 17,400 lb. 12,000 lb = $K^2W_m = (4.29)^2\ W_m$ and 17,400 lb = $K^2W_m = (5.17)^2\ W_m$. Although 4.29 is the geometrically correct weight scaling factor, 5.17 provides a sinkage factor in CH soil that is closer to a 4.29 value for the sinkage factor. A sinkage factor of $k_n = 4.29$ for Z_p/Z_m means that $Z_p/d_{w_p} = Z_m/d_{w_m}$* for the prototype-model geometric scale factor used in this series of tests. The CL soil does not follow the same relationships as the other two soils, possibly due to the extreme stratification effects encountered in this low permeability soil.

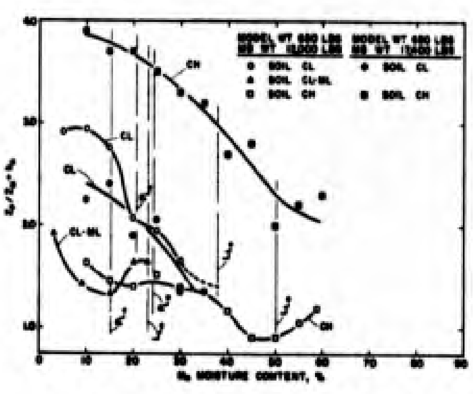

FIGURE 46. SINKAGE SCALING FACTOR FOR THE THREE TEST SOILS

*See page 44, Equation (4).

GENERAL DISCUSSION

A study of the data generated and the experience in testing techniques accumulated during this project in all three soils established the following points:

(1) "In situ" (untilled) soil testing is of little or no value for scale-model testing due to nonhomogeneity of the soil. Stratification due to variation in compaction of the soil, difficulty in obtaining homogeneous distribution of the moisture throughout the soil depth, and the variation in soil strength as a result of the roots from vegetation that has been cleared from the surface of the soil cause the soil to have a range of soil strength as a function of depth. The depth of the soil layer thus becomes quite significant and would introduce another strong, independent, nonreproducible and random parameter into an already complex problem area.

(2) Thoroughly disaggregated soil provided the most consistent and repeatable test results. Final tilling must be accomplished immediately before adding moisture to prevent stratification as a result of differential compaction as a function of soil depth.

(3) One test run renders a prepared test course completely unsuitable for further testing until it is thoroughly reconditioned. Reconditioning of the test course cannot be accomplished properly until the test course has dried out sufficiently to permit the gyrotiller to retill and disaggregate the soil without "balling it up" in big clods. The soil must be sufficiently dry to be friable; otherwise, there is excessive nonhomogeneity. As much as 10,000 to 15,000 gallons of water must be evenly and carefully distributed on one test course to prepare it for a single pass of the Marsh Buggy. The logistics of this type of effort are considerable.

(4) The drawbar pull of any test vehicle is not affected by the forward velocity of the vehicles in the practical speed ranges of the vehicles used during these tests. Grouser-tired vehicles will dig in at high slip and low forward velocities much more so than at low slip and higher speeds. Excellent repeatability and correlation between model and prototype for D/W versus the percent of slip can be obtained at certain ranges of moisture content in all types of soil.

(5) Good repeatability of all soil characteristics as a function of moisture content is difficult to obtain throughout the complete range of moisture levels tested. This is due largely to the heterogeneous soil characteristics of "average" disaggregated soils and the difficulty in obtaining "representative" soil samples and a uniform distribution of moisture. Changes of soil characteristics with changes in moisture content are measurable by all the test techniques reported herein; however, the soil frictional characteristics prove to be the most accurate correlating factor for the prediction of vehicle performance.

(6) At certain moisture content ranges, the high-cohesion soil, CH, tended to adhere to the surface of the tire. This changed b, the tire width; d_w, the tire diameter; and Z, the tire sinkage. The soil sticking to the tire surface acted much as grousers and literally ripped up the test course in deep, wide furrows. This made actual determination of the test variables such as sinkage, slip, and drawbar pull difficult to measure accurately. Medium-cohesion soil presents similar characteristics to a lesser degree at certain moisture contents, whereas predominately sandy-type soils indicate no appreciable adhesion to the tires.

(7) All soils tested show definite and abrupt changes in characteristics with changes of small percentages of moisture content at certain critical levels. This is especially noticeable at or near the liquid limits of all three test soils, and this results in abrupt decreases in drawbar pull and abrupt increases of tire sinkage for all vehicles tested in all three types of soils.

CONCLUSIONS AND OBSERVATIONS

1. Satisfactory correlation between full-scale vehicle drawbar pull and model drawbar pull can be accomplished through the use of suitable scaling factors. The correlation is acceptable over a wide range of soil cohesion and moisture content. Soil friction is the most important soil parameter for predicting vehicle performance. The closest correlation of D/W between prototype and model is obtained in clay soils with the soil of the highest plasticity index and at a moisture content level where D/W versus M_n has the minimum slope.

2. The modeling technique does not appear to correlate the sinkage response parameter, Z/d_w, when the correct weight scaling factor, $(4.29)^2$, is used. By using a distorted weight scaling factor it appears to be possible in some soils to correlate the sinkage response parameter, Z/d_w, so that $\frac{Z_p}{d_{w_p}} = \frac{Z_m}{d_{w_m}}$. The need for a distorted weight scaling factor may result from the inability to "scale" the test soil.

3. Improved soil testing equipment must be designed and evaluated. The rotating rubber-faced plates developed for this program for determining f_n, the coefficient of friction of the soil, is a step in the correct direction, but the test procedure and instrumentation require refinement and development. It is felt that a significant "breakthrough" has been accomplished by this program in correlating the D/W test results as a function of the moisture content of the soil and in comparing these results to the corresponding f_n or coefficient of friction of the soil at that particular moisture content. This method of plotting the test results has defined surprising "peaks" in the D/W values at certain values of the moisture content that were not capable of definition through the use of previous soil parameters.

RECOMMENDATIONS FOR FURTHER RESEARCH

It is recommended that the present research be continued to further perfect the modeling technique for predicting vehicle performance by employing the following measures:

(1) A full-scale vehicle with higher drawbar pull potential is needed. The Marsh Buggy could not develop maximum drawbar pull at many soil conditions due to failure of its drive chains. The full-scale vehicle should be capable of using a number of different types of tires in a wide range of cohesive soils. The vehicle should have a limited slip differential or should be operated on the test course with a locked differential.

(2) The adhesion of high-cohesion clays at certain moisture contents should be thoroughly investigated. The influence of the effect of adhesion on drawbar pull is clearly shown in Figures 43 through 45. This is a significant factor that strongly influences the drawbar performance of vehicles. An improved means of defining the adhesion properties of the soils is needed. By suitable modification of f_n by some adhesion factor, it should be possible to improve the correlation shown in Figures 43 through 45. It is believed that the insertion of a plate or several plates edgewise into the soil and their subsequent withdrawal will provide a level of information not now available. The force required to withdraw the plates (the adhesion shear developed) plus the added information provided by the gain in static weight of the plates due to the adhesion of soil to the plates should provide new soil parameters that will more accurately describe the adhesion phenomenon that is now occurring and its effect on drawbar pull.

(3) The coefficient of friction of the soil, f_n, needs detailed study for improved instrumentation. It is felt that a 1- to 2-inch strip of rubber-faced steel plate should be used on a 12- to 18-inch center to form a hollow circle. The support of this circular strip should be such that it will minimize edge effects and pickup due to plastic flow of the mud up and over the edges of the strip. Perhaps scrapers or cleaners should be used to remove the mud buildup on top of the strip due to the plastic flow. The circular strip should be capable of rotation at varying rates of peripheral speed to simulate varying slip ratios, and the unit loading should be capable of variation over a realistic range of values. The torque measurement on this equipment should be sensitive over a wide range of torque values and should possibly have a selective range scale. It may be desirable to investigate the effect of grousers on this rubber-faced strip. Loading up of these grousers by the adhesion of the soil to produce pure friction loading should establish where this effect will occur in full-scale tires.

(4) Study and correlation of the sinkages of the prototype and model should be continued. The correction factor, k_n, appears to correlate the model and prototype in the permeable soils, but it appears that some additional factor should be introduced to permit a "corrected k_n" to be a constant value regardless of moisture content or soil composition.

BIBLIOGRAPHY

Capper, P. Leonard and Cassie, W. Fisher, The Mechanics of Engineering Soils, Second Edition, McGraw-Hill Book Company, Inc., New York, New York, 1953, pp. 28-121.

Creech, Merl D., "Dimensional Analysis," Part VI, Product Engineering, Volume 33, No. 21, October 15, 1962, pp. 139-142.

Harrison, W. L., et al., A Soil Value System for Land Locomotion Mechanics, Land Locomotion Research Branch Report No. 5, Department of the Army, Ordnance Tank-Automotive Command, Centerline, Michigan, December 1958, pp. 34-42 and 79-89.

Langhaar, Henry L., Dimensional Analysis and Theory of Models, John Wiley & Sons, Inc., New York, New York, 1951, pp. 18-20 and 34-41.

Murphy, Glenn, Similitude in Engineering, The Ronald Press Company, New York, New York, 1950, pp. 57-72.

Nuttall, C. J., Jr. and McGowan, Robert P., Scale Models of Vehicles in Soils and Snow, TREC Technical Report 61-50, U. S. Army Transportation Research Command, Fort Eustis, Virginia, June 1961, pp. 5-14.

Roma, Carlo J. and McGowan, Robert P., Scaled Vehicle Mobility Factors (Tires in Sand), TREC Technical Report 61-49, U. S. Army Transportation Research Command, Fort Eustis, Virginia, April 1961, pp. 11-33.

Roma, Carlo J. and McGowan, Robert P., Scaled Vehicle Mobility Factors (Scale Model Tires in Snow), TREC Technical Report 61-118, U. S. Army Transportation Research Command, Fort Eustis, Virginia, October 1961, pp. 10-35.

Wilson, Nuttall, and Raimond, Scaled Vehicle Mobility Factors (Sand), TREC Technical Report 61-67, U. S. Army Transportation Research Command, Fort Eustis, Virginia, April 1961, pp. 30-44.

BLANK PAGE

APPENDIX I

TABLE I
CHARACTERISTICS OF TEST TIRES

	M.B. Std.	M.B. Smt.	M.B. Model	LCC Model	Truck, 3/4-Ton
O.D., In. (d_w)	114.7	60.7	25.9	28.0	35.5
Width, In. (b)	38.5	18.6	9.0	12.0	10.5
Rim, In.	66	25	14	17	16
Section Height, In.*	22.5	16.4	5.1	6.1	8.2
Tread Depth, In.	Smooth	1/2	Smooth	1/4	5/8
Ply	8	12	2	6	8
Load/Tire - lb. (avg.)	3000	2660	162	250	1570
Ground Press, psi**	8.0	14.5	4.5	6.2	31

*Measured from rim flange to outside diameter of undeflected tire.
**Calculated from weight per tire and contact print of tire at zero sinkage and average tire pressures.

TABLE II
TYPICAL VEHICLE TEST RESULTS

Vehicle	Weight, lb.	Soil	M.C., %	Slip, %	D/W	Z, in.
M.B. (Std. Tires)	12,000	CH	35	20	.60	2
			45	60	.20	3
			55	80	.10	8
			41	30	.55	6
			62	82	.07	11
			34	8	.56	2
			47	80	.06	19
			47	87	.19	16
			66	75	.14	18
			37	41	.59	3
			22	65	.36	2
			40	55	.26	2
			43	55	.33	3
			56	76	.29	5
			57	80	.49	6
			51	50	.56	6
			51	17	.52	5
			22	60	.37	2
			58	43	.09	9
M.B.	12,000	CL	38	65	.40	6
			38	25	.32	5
			23	10	.50	3
			23	25	.52	3
			10	12	.34	3
			39	44	.28	6
M.B.	12,000	CL-ML	24	75	.18	10
			22	81	.22	4
			20	75	.19	3
			21	67	.07	7
			24	85	.09	7
			27	70	.12	13
			7	50	.42	4
			15	30	.38	2
			5	35	.42	4
			25	55	.32	3
			16	60	.30	3
M.B. (Sandmaster Tires)	10,640	CH	32	50	.62	4
			32	80	.75	5
			26	7	.54	2
			26	40	.54	6
			40	15	.42	5
			40	90	.53	14
			49	83	.36	8
			55	83	.06	14
			36	75	.60	6
M.B. (Sandmaster Tires)	10,640	CL	33	70	.23	5
			15	35	.45	3
			15	75	.57	4
			28	62	.49	5

TABLE II (Cont'd)
TYPICAL VEHICLE TEST RESULTS

Vehicle	Weight, lb.	Soil	M.C., %	Slip, %	D/W	Z, in.
M.B. (Sandmaster Tires)	10,640	CL-ML	6	41	.31	5
			9	79	.48	6
			8	40	.37	3
			8	56	.47	4
			30	93	.15	16
M.B.	13,800	CH	52	71	.07	13
		CL	33	10	.30	4
		CL	9	45	.42	3
		CL-ML	20	20	.36	4
		CL-ML	7	28	.36	5
		CL-ML	2	15	.36	4
M.B.	15,600	CH	47	83	.12	17
		CL	33	10	.33	1
		CL	29	15	.39	2
		CL-ML	9	20	.39	3
		CL-ML	21	70	.12	10
		CL-ML	8	70	.21	5
M.B.	17,400	CH	48	66	.23	9
		CL	25	10	.35	3
		CL	40	70	.23	9
		CL-ML	6	10	.28	2
M.B. Model	650	CH	24	28	.29	1
			24	57	.37	2
			37	27	.38	1
			37	42	.24	1
			50	70	.18	2
			44	56	.42	1
			44	27	.81	1
			53	40	.14	6
M.B. Model	400	CL	10	55	.23	3
	565	CL	15	15	.32	2
	565	CL	14	70	.44	2
	650	CL	10	17	.35	1
	650	CL	2	55	.43	3
	650	CL	11	55	.43	3
	650	CL-ML	13	20	.27	2
	650	CL-ML	13	70	.39	3
	650	CL-ML	6	40	.39	3
	650	CL-ML	2	25	.43	3
	650	CL-ML	20	70	.43	3
	400	CL-ML	14	50	.34	1
	400	CL-ML	13	20	.27	2
	565	CL-ML	6	25	.38	3
	565	CL-ML	20	25	.37	2

TABLE II (Cont'd)
TYPICAL VEHICLE TEST RESULTS

Vehicle	Weight, lb	Soil	M.C., %	Slip, %	D/W	Z, in.
LCC Model	1,000	CH	14	70	.50	1
	1,000	CH	53	70	.37	6
	1,000	CL	7	60	.42	2
	2,000	CL	20	50	.62	2
	2,000	CL	10	10	.50	3
	1,000	CL-ML	7	30	.75	2
	1,000	CL-ML	15	70	.82	2
Truck 3/4-Ton	6,300	CL	7	20	.25	3
			7	80	.31	4
			35	20	.05	6
			35	80	.11	7
		CL-ML	7	30	.30	4
			7	80	.39	6
			22	80	.11	12

APPENDIX II - SIMILITUDE ANALYSIS

THEORY OF SIMILITUDE IN THE USE OF MODELS

Modern engineering practice relies heavily upon the use of models to predict the full-scale vehicle performance of expensive prototype designs. The principles which underlie the proper construction, design, scale considerations, design of experiment, and the interpretation of the test results involving the use of models comprise the theory of similitude. The theory of similitude includes a consideration of the conditions under which the behavior of two separate systems will be similar, and the techniques of accurately predicting results on the one from the analysis and interpretation of the observations on the other.

From a series of carefully selected observations of an intelligently planned series of experiments, there may be established a repeatable and reproducible set of relations between the variables which is sufficiently general to permit predictions with an acceptable degree of accuracy.

There are three classes of models normally employed:

(1) Geometrically similar. The model is a scale reproduction of the prototype.

(2) Distorted. The model is a reproduction of the prototype, but two or more different scales are used. The length may be one scale and the width a second scale.

(3) Dissimilar. There is no direct resemblance between the model and the prototype.

In the present study, the geometrically similar model was employed. That is, if the subscript p refers to the full-size vehicle and the subscript m refers to the model, then the relation between any pertinent dimensions on the full-scale prototype and the model is such that

$$\frac{P_p}{P_m} = \frac{Q_p}{Q_m} = \ldots\ldots = \frac{X_p}{X_m} = \frac{Y_p}{Y_m} = K$$

where K is a constant equal to the ratio of the pertinent dimensions of or between similar components on the full-scale prototype vehicle and the model.

The theory of similitude serves not only to establish those relations necessary to permit reliable predictions to be made from observation of experiments conducted with the model but also to establish the type of relationship existing among the parameters involved in the physical phenomenon of interest, so that through logical planning only pertinent data will be generated during the test program.

The theory of similitude is developed by the use of dimensional analysis, since that procedure offers the most general approach to the study of any physical phenomenon. Dimensional analysis can be a strong analytical tool when properly applied. Its usefulness in the solution of a complex problem, however, is dependent upon the degree of knowledge or understanding by the analyst of the physical phenomenon under investigation. Dimensional analysis is concerned with the dimensions in which each of the pertinent variables in a physical phenomenon is expressed. It is based on the following two axioms:

<u>Axiom I</u>: Absolute numerical equality of quantities may exist only when the quantities are similar qualitatively.

<u>Axiom II</u>: The ratio of the magnitudes of two like quantities is independent of the units used in their measurement, provided that the same units are used for evaluating each quantity.

In our present problem, in which soil and vehicles are involved, our similarity requirements must involve all of the significant parameters of the soils and the vehicles, and we must determine that all of the effects of the various parameters are correctly scaled between the prototype and the model. Similarity requires maintenance of equality among all of the important ratios of effects in model and in prototype.

To express or compare the equality of these important ratios of effects between prototype and model, we must develop an appropriate set of dimensionless quantities. The determination of an appropriate set of dimensionless quantities to be used in our similitude study must be directed by the selection of only those parameters determined to be significant to this problem. It is necessary that these parameters form a complete set in that the problem is fully defined by the selected parameters and a unique relationship exists. When this unique functional relationship is not known or not fully understood, as in the present problem, we can utilize the Buckingham Pi Theorem to generate a set of dimensionless parameters from combinations of the original dimensional parameters.

The Buckingham Pi Theorem states that the number of dimensionless and independent quantities required to define a relationship among the variables in a specific physical phenomenon is equal to the number of quantities involved minus the number of dimensions in which those quantities may be measured. Therefore, the Pi Theorem states

$$S = n - b$$

where

S = number of π terms

n = total number of quantities involved

b = the number of basic dimensions involved

If the equation represented by the unknown function $f = (\alpha, \beta, \gamma, \ldots\ldots) = 0$ is a complete equation and $\alpha, \beta, \gamma, \ldots.,$ etc., are physically measurable quantities defining the phenomenon under investigation, then it is possible to form a function of independent dimensionless products

$$F = (\pi_1, \pi_2, \pi_3, \ldots\ldots, \pi_{m-b}) = 0$$

where m is the number of measurable quantities and dimensional constants and b is the number of primary dimensions involved.

The π theorem now permits us to write

$$\pi_1 = f(\pi_2, \pi_3, \ldots\ldots, \pi_S)$$

The relationship between a model and the prototype may now be expressed as

$$\frac{\pi_{1_p}}{\pi_{1_m}} = \frac{f(\pi_{2_p}, \pi_{3_p}, \ldots\ldots, \pi_{S_p})}{f(\pi_{2_m}, \pi_{3_m}, \ldots\ldots, \pi_{S_m})}$$

where the subscripts p and m designate the prototype and the model, respectively.

The model must be designed and operated so that

$$\pi_{2_m} = \pi_{2_p}$$

$$\pi_{3_m} = \pi_{3_p}$$

$$\pi_{4_m} = \pi_{4_p}$$

$$\ldots\ldots$$

$$\pi_{S_m} = \pi_{S_p}$$

It follows that

$$f(\pi_{2_p}, \pi_{3_p}, \ldots\ldots, \pi_{S_p}) = f(\pi_{2_m}, \pi_{3_m}, \ldots\ldots\ldots, \pi_{S_m}),$$

and it is apparent that

$$\pi_{1_p} = \pi_{1_m}$$

SELECTION OF SIGNIFICANT PARAMETERS

VEHICLE PARAMETERS OR FACTORS

1. d_w = Wheel diameter of vehicle. The tractive element that will be in contact with the soil.

2. V = Forward velocity of the vehicle relative to an axis fixed in the surface of the soil.

3. V_s = Peripheral velocity of the wheel relative to an axis fixed on the vehicle.

4. S = Slip ratio $= \dfrac{V_s - V}{V_s}$

5. W = Vehicle weight.

6. δ = Tire deflection $= 1 - \dfrac{(\text{Deflected Section Height})}{(\text{Undeflected Section Height})}$

   Deflected section height is the vertical distance from the rim flange to a hard surface. Undeflected section height is the distance measured in a radial direction from the rim flange to the outermost undeflected surface of the tire; all measurements are unique for a given tire inflation pressure.

7. b = Tire width at design inflation pressure.

SOIL PARAMETERS OR FACTORS

8. h = Depth of homogeneous soil.

9. C_s = Precollapse structural cohesion, psi.

10. C_t = Postcollapse structural cohesion at depth h_i, psi.

11. C_r = Apparent structural cohesion, psi. This factor is empirically determined and is "modeled" to the tire footprint.

12. ϕ = Angle of internal friction.

13. τ = Dynamic shearing stress. This is approximated by Coulomb's equation:

$$\tau = C_s + \sigma(\tan \phi).$$

where σ = unit normal loading on the shear plane.

14. A = Slope of soil surface.

15. f_n = Coefficient of friction between tractive surface and soil at soil condition, n.

16. β_n = Plastic kinematic viscosity of soil at condition, n.

17. γ_n = Specific weight of soil at condition n.

18. M_n = Moisture content $= \frac{W_e}{W_s}$, at condition n,

where

W_e = wt. of liquid in a unit volume,

W_s = wt. of solids in the unit volume.

DEPENDENT VARIABLES (RESPONSE PARAMETERS)

19. Z = Sinkage of vehicle.

20. D = Drawbar pull of vehicle.

The investigation of 19 independent and 2 dependent variables would be a time-consuming task that would not be justified for the results that would possibly be obtained. The two important parameters that must be investigated relative to the performance of the full-scale vehicle and models in the clay soils of varying levels of moisture content are the two dependent variables: Z = sinkage of the vehicle, and D = drawbar pull of the vehicle. Z is important in vehicle design because adequate ground clearance must be maintained during operation in traversing difficult soils. D is of prime importance because it is necessary to know what useful work can be accomplished by the vehicle in towing additional equipment or, in the case of a single vehicle, what margin of safety is available over and above the tractive effort required to propel the vehicle through difficult terrain conditions.

The review of prior work in this field, particularly the investigations conducted by TRECOM, indicates that satisfactory correlation between model and full-scale vehicle performance can be accomplished by ignoring the minor effects of some of the variables so that the investigation can be simplified and shortened. It is extremely important to eliminate all minor or insignificant parameters, since each significant independent variable must be investigated through a range of realistic values while all other independent variables are held constant.

Let us examine each variable separately to determine its relative significance to the final solution so that we may reduce the number of terms that must be investigated:

d_w = Wheel diameter of vehicle. This is an important independent variable since it affects the ground contact area of the vehicle.

V = Forward velocity of the vehicle. At the slow speeds to be investigated for this similitude study, it has been established empirically by a number of investigators in snow, sand, and soil that velocity effects and the influence of velocity-dependent variables are negligible with respect to the response parameters of interest. However, these considerations will be incorporated into the analysis until it can be definitely established that their effect is negligible for the clay soils.

V_s = Peripheral velocity of the wheel with respect to an axis fixed on the vehicle. It has been determined empirically that V_s is not significant as an independent variable with respect to the response parameters.

S = Slip ratio = $\frac{V_s - V}{V_s}$. The slip ratio is a significant parameter. This fact has been established in prior investigations.

W = Vehicle weight. This is a significant parameter. The study concerns four-wheeled vehicles with four equally loaded tires; therefore, we may merely consider the gross weight of the vehicle in the analysis.

δ = Tire deflection. This is a significant parameter since the contact area of the tire with the ground is a function of the tire deflection. Tire deflection can be maintained as a constant for a series of different vehicle weights by varying the tire inflation pressure.

b = Tire width at design inflation pressure. This is an important parameter since it affects the ground contact area of the vehicle. The ground contact area $\cong b\ell_w$.

h = Depth of homogeneous soil. In field tests, it will not be possible to scale the depth of the homogeneous soil for prototype and model, so it will be necessary to use a depth of soil sufficiently deep as to be considered a semi-infinite mass so that the effect of h will not be significant.

C_s = Precollapse structural cohesion, psi. This is a significant soil parameter. Strength is the shear of the undisturbed soil.

C_t = Postcollapse structural cohesion, psi. As the wheel crushes the soil, consolidation occurs under the wheel contact area. Strength is shear of compressed soil.

C_r = Apparent structural cohesion, psi. This has been determined empirically as being an important soil parameter. It is a measure of the sinkage of "modeled" plate diameters under normal loading.

ϕ = The angle of internal friction. This is an important parameter, a measure of the soil's internal friction.

τ = Dynamic shearing stress. $\tau = C_s + \sigma(\tan \phi)$; therefore, τ may be expressed in terms of C_s or C_t and ϕ.

A = Slope of surface. To simplify this similitude study, all field testing will be accomplished on level ground.

f_n = Coefficient of friction between the tractive element and soil at soil condition n. This is an important parameter for the clay soils.

μ_n = Plastic viscosity of soil at condition n. Initially the viscosity of the soil will be included in the analysis unless it is established definitely that velocity effects are negligible.

γ_n = Specific weight of soil at condition n. Initially the specific weight of the soil will be included unless it is established definitely that inertia effects are negligible at low forward velocities.

M_n = Moisture content of soil = W_e/W_s. This is an important parameter since it will influence the coefficient of friction in certain soils.

Z = Sinkage of vehicle. This is a basic response parameter.

D = Drawbar pull. This is a basic response parameter.

Therefore,

$$f(d_w, V, S, W, \delta, b, C_r, C_t, C_s, \phi, f_n, \beta_n, \gamma_n, M_n, Z, D) = 0$$

We have 3 basic dimensions: F, L, and T. We have 16 measurable quantities; we therefore have 13 π terms or nondimensional quantities involved in the relationship between the variables in the physical phenomenon.

1.	d_w	= L	6.	b	= L	11.	f_n	= - (Ratio)
2.	V	= LT^{-1}	7.	C_r	= FL^{-2}	12.	β_n	= $FL^{-2}T$
3.	S	= - (Ratio)	8.	C_t	= FL^{-2}	13.	γ_n	= FL^{-3}
4.	W	= F	9.	C_s	= FL^{-2}	14.	M_n	= - (Ratio)
5.	δ	= - (Ratio)	10.	ϕ	= - (Ratio)	15.	Z	= L
						16.	D	= F

The following simultaneous equations can then be written:

$$F:\ C_4 + C_7 + C_8 + C_9 + C_{12} + C_{13} + C_{16} = 0 \quad (1)$$

$$L:\ C_1 + C_2 + C_6 - 2C_7 - 2C_8 - 2C_9 - 2C_{12} - 3C_{13} + C_{15} = 0 \quad (2)$$

$$T:\ -C_2 + C_{12} = 0 \quad (3)$$

Since there are 3 equations available for the solution of 11 unknowns, we must assign arbitrary values to 8 of the unknowns. C_1, C_2, C_6, C_7, C_8, C_{13}, C_{15}, and C_{16} will be selected. The determinant of the coefficients of the remaining terms (C_4, C_9, C_{12}) is:

$$\begin{vmatrix} 1 & 1 & 1 \\ 0 & -2 & -2 \\ 0 & 0 & 1 \end{vmatrix} = -2$$

This is not equal to zero, so the selection is valid, and the resulting equations are independent.

Substituting in the simultaneous equations and solving, we obtain the following π terms:

$$\pi_1 = \frac{W}{d_w^2 C_s} \qquad \pi_3 = \frac{W}{b^2 C_s} \qquad \pi_5 = \frac{C_t}{C_s}$$

$$\pi_2 = \frac{W C_s}{\beta_n^2 V^2} \qquad \pi_4 = \frac{C_r}{C_s} \qquad \pi_6 = \frac{\gamma_n^2 W}{C_s^3}$$

$$\pi_7 = \frac{ZC_s^{1/2}}{W^{1/2}} \qquad \pi_9 = S \qquad \pi_{11} = \phi$$

$$\pi_8 = \frac{D}{W} \qquad \pi_{10} = \delta \qquad \pi_{12} = f_n$$

$$\pi_{13} = M_n$$

The π terms may be multiplied or divided by other π terms to provide new π terms to replace the old ones. The resulting final π terms are as follows:

$$\pi_1 = \frac{W}{bd_wC_s} \qquad \pi_5 = \frac{\gamma_n b}{C_t} \qquad \pi_9 = S$$

$$\pi_2 = \frac{\beta_n V}{bC_s} \qquad \pi_6 = \frac{\gamma_n b}{C_r} \qquad \pi_{10} = \delta$$

$$\pi_3 = \frac{W}{b^2C_s} \qquad \pi_7 = \frac{Z}{d_w} \qquad \pi_{11} = \phi$$

$$\pi_4 = \frac{C_r}{C_t} \qquad \pi_8 = \frac{D}{W} \qquad \pi_{12} = f_n$$

$$\pi_{13} = M_n$$

The final π terms include the load numerics, π_1 and π_3, and the response parameters, π_7, π_8.

Our modeling criterion, i.e., the criterion for exact similitude, states that all dimensionless parameters must be maintained equal for the model and the prototype. Due to the fact that the models furnished for this test have a scale of 1/4.29, and the requirement that we have to employ the same soils for model and prototype tests, we do not always have complete freedom in choosing the combinations to maintain equality of π terms.

For similitude,

$$\pi_{1_p} = \pi_{1_m}$$

subscripts p = prototype
m = model

$$\frac{W_p}{b_p d_{w_p} C_{s_p}} = \frac{W_m}{b_m d_{w_m} C_{s_m}}$$

By definition,

$$b_p = Kb_m$$

$$d_{w_p} = Kd_{w_m}$$

$$C_{s_p} = C_{s_m}$$

Substituting and solving,

$$W_p = K^2 W_m$$

$$\pi_{2_p} = \pi_{2_m}$$

$$\frac{\beta_{n_p} V_p}{b_p C_{s_p}} = \frac{\beta_{n_m} V_m}{b_m C_{s_m}}$$

$$b_p = K b_m;$$

and if we assume that

$$V_p = K V_m,$$

then

$$\frac{\beta_{n_p} K V_m}{K b_m C_{s_m}} = \frac{\beta_{n_m} V_m}{b_m C_{s_m}}$$

and

$$\beta_{n_p} = \beta_{m_p}$$

For π_3 the results are identical to π_1, and

$$W_p = K^2 W_m$$

$$\pi_{4_p} = \pi_{4_m}$$

$$\frac{C_{r_p}}{C_{t_p}} = \frac{C_{r_m}}{C_{t_m}}$$

$C_{r_p} = K C_{r_m}$, by definition of C_r, since C_r is a "modeled" soil parameter.

Then

$$\frac{K C_{r_m}}{C_{t_p}} = \frac{C_{r_m}}{C_{t_m}}$$

$$C_{t_p} = K C_{t_m}$$

$$\pi_{5_p} = \pi_{5_m}$$

$$\frac{\gamma_{n_p} b_p}{C_{t_p}} = \frac{\gamma_{n_m} b_m}{C_{t_m}}$$

$$b_p = Kb_m \text{ and } C_{t_p} = KC_{t_m}$$

then

$$\frac{\gamma_{n_p} Kb_m}{KC_{t_m}} = \frac{\gamma_{n_m} b_m}{C_{t_m}}$$

and

$$\gamma_{n_p} = \gamma_{n_m}$$

$$\pi_{6_p} = \pi_{6_m}$$

$$\frac{\gamma_{n_p} b_p}{C_{r_p}} = \frac{\gamma_{n_m} b_m}{C_{r_m}}$$

$$b_p = Kb_m \text{ and } C_{r_p} = KC_{r_m}$$

then

$$\frac{\gamma_{n_p} Kb_m}{KC_{r_m}} = \frac{\gamma_{n_m} b_m}{C_{r_m}}$$

and

$$\gamma_{n_p} = \gamma_{n_m}$$

π_7 and π_8 are response parameters, so if all other terms are properly modeled, then

$$\pi_{7_p} = \pi_{7_m} \text{ and } \pi_{8_p} = \pi_{8_m}$$

However, for reference in conducting the experimental work, it is helpful to know the following relations:

$$\pi_{7_p} = \pi_{7_m}$$

$$\frac{Z_p}{d_{w_p}} = \frac{Z_m}{d_{w_m}}$$

$$d_{w_p} = Kd_{w_m}$$

$$\frac{Z_p}{Kd_{w_m}} = \frac{Z_m}{d_{w_m}}$$

and

$$Z_p = KZ_m$$

$$\pi_{8_p} = \pi_{8_m}$$

$$\frac{D_p}{W_p} = \frac{D_m}{W_m}$$

From π_1,

$$W_p = K^2 W_m$$

$$\frac{D_p}{K^2 W_m} = \frac{D_m}{W_m}$$

and

$$D_p = K^2 D_m$$

$$\pi_{9_m} = \pi_{9_p}$$

$$S_m = S_p$$

$$\frac{V_{s_p} - V_p}{V_{s_p}} = \frac{V_{s_m} - V_m}{V_{s_m}}$$

Since we previously assumed

$$V_p = KV_m$$

$$\frac{V_{s_p} - KV_m}{V_{s_p}} = \frac{V_{s_m} - V_m}{V_{s_m}}$$

and $V_{s_p} = KV_{s_m}$

$$\pi_{10_p} = \pi_{10_m}$$

$$\delta_p = \delta_m$$

By the geometric similitude of the model and the prototype,

$$\frac{\delta_p}{\delta_m} = 1$$

$$\pi_{11_p} = \pi_{11_m}$$

$$\phi_p = \phi_m$$

and

$\phi_p/\phi_m = 1$ because the soil will not be scaled.

$$\pi_{12_p} = \pi_{12_m}$$

and $f_{n_p} = f_{n_m}$ by definition of the soil.

$$\pi_{13_p} = \pi_{13_m}$$

$$M_{n_p} = M_{n_m}$$

and $M_{n_p}/M_{n_m} = 1$ by definition of the soil.

In summation, the modeling requirements for geometric similitude must be such that:

(1) $W_p = K^2 W_m$

where $K = 4.29$

$W_p = 18.4 W_m$.

(2) If we assume

$V_p = KV_m$

then,

$\beta_{n_p} = \beta_{n_m}$

(3) $\gamma_{n_p} = \gamma_{n_m}$

(4) $Z_p = KZ_m = 4.29 Z_m$

(5) $D_p = K^2 D_m = 18.4 D_m$

(6) If $V_p = KV_m$

then $V_{s_p} = KV_{s_m} = 4.29 V_{s_m}$

The π terms selected are not a unique set of relations. A variety of new π terms are possible by the manipulation of the present terms. These terms were selected to avoid the generation of any term that would require scaling of the soil (an impossibility for this type of investigation). By scaling the velocity of the vehicles, it is possible, as indicated by this analysis, to avoid the scaling of β_n, the viscosity of the soil. Test results indicate, however, that, for the low range of velocities employed in this analysis, the effect of velocity is negligible; therefore, $\beta_{n_p} = \beta_{n_m}$ for these low velocities.